RESEARCH ARTICLE

Collagen Restoration from Combined Radiofrequency Microneedling and Polydioxanone Filler in Oxidative Stress-Mediated Skin Aging

Ruth Agustina Sinaga[1], Cindra Paskaria[2], Wahyu Widowati[1,2,*]

[1]Master Program of Skin Ageing and Aesthetic Medicine, Faculty of Medicine, Maranatha Christian University, Jl. Prof. drg. Surya Sumantri, M.P.H. No. 65, Bandung 40164, Indonesia
[2]Department of Pharmacology, Faculty of Medicine, Maranatha Christian University, Jl. Prof. drg. Surya Sumantri, M.P.H. No. 65, Bandung 40164, Indonesia

*Corresponding author. Email: wahyu.widowati@maranatha.edu

Received date: Jan 28, 2026; Revised date: Mar 13, 2026; Accepted date: Mar 16, 2026

Abstract

BACKGROUND: Oxidative stress plays a central role in skin aging by promoting reactive oxygen species–mediated collagen degradation, fibroblast senescence, and dermal thinning. Although radiofrequency microneedling (RFM) and polydioxanone (PDO) filler individually stimulate collagen remodeling, evidence regarding their combined efficacy in oxidative stress induced skin aging models remains limited. This study evaluated the effects of combined RFM and PDO filler therapy in a D-galactose–induced oxidative stress model of skin aging.

METHODS: Thirty female Sprague-Dawley rats were randomly assigned into five groups (n=5): normal control (NC), aging control (AC), RFM monotherapy, PDO monotherapy, and combination therapy. Oxidative aging was induced by daily intraperitoneal injections of 50 mg/kg for 8 weeks, followed by a single post-induction treatment session. Skin samples were collected at 12 weeks post-treatment for histological assessment of dermal thickness (hematoxylin–eosin), collagen density (Masson's trichrome), and fibroblast count.

RESULTS: D-galactose significantly reduced dermal thickness, collagen density, and fibroblast count in AC compared with NC (p<0.001). All treatment groups showed significant improvement versus AC (p<0.05). Notably, only the combination therapy restored collagen density to a level comparable with normal skin (35.22 [28.74–40.35]% *vs.* 37.83 [33.11–40.69]%, p=0.124). The combination group also showed the highest increases in dermal thickness and fibroblast numbers among treatment groups.

CONCLUSION: In this preclinical model, combined RFM and PDO filler therapy demonstrated enhanced restoration of dermal structure and collagen under oxidative stress–mediated skin aging, supporting its potential role in skin rejuvenation strategies.

KEYWORDS: collagen density, dermal regeneration, D-galactose, oxidative stress, skin aging

Indones Biomed J. 2026; 18(2): 173-82

Introduction

The development of effective, minimally invasive interventions for cutaneous aging remains a key focus in dermatologic and aesthetic medicine.(1) Skin aging is characterized by progressive structural and functional deterioration, including reduced dermal thickness, decreased collagen density, and fibroblast depletion, which contribute to loss of elasticity and impaired regenerative capacity.(2) These changes are largely driven by oxidative stress, which promotes reactive oxygen species production, cellular senescence, and degradation of extracellular matrix components. In addition to extrinsic aging caused by ultraviolet radiation, intrinsic aging can be studied using systemic oxidative stress models such as D-galactose induction, which accelerates aging through advanced glycation end-product accumulation, mitochondrial

Copyright © 2026 The Prodia Education and Research Institute.
This work is licensed under a Creative Commons Attribution-NonCommercial 4.0 International (CC-BY-NC) License.

dysfunction, and collagen degradation.(3-5) This model provides a controlled experimental platform to evaluate therapeutic strategies targeting oxidative stress–mediated dermal degeneration.

Radiofrequency microneedling (RFM) and polydioxanone (PDO) filler are widely used collagen-stimulating treatments with demonstrated regenerative potential. RFM induces controlled microthermal injury, activating wound-healing pathways that promote fibroblast proliferation, neocollagenesis, and dermal remodeling. (6,7) Histological studies have shown that RFM increases collagen types I and III and improve dermal architecture in aging skin. Meanwhile, PDO filler acts as a biodegradable biostimulatory scaffold that stimulates fibroblast recruitment and sustained collagen synthesis, thereby improving dermal structure and tissue integrity.(8,9) Both treatments have demonstrated effectiveness as monotherapies in improving structural and cellular features of aged skin.

Combination therapies that target multiple regenerative mechanisms are increasingly investigated to enhance treatment efficacy and durability.(10,11) RFM may enhance dermal permeability, stimulate early regenerative signaling, and improve the tissue microenvironment, while PDO filler provides structural support for sustained extracellular matrix regeneration.(12) These complementary mechanisms suggest that combined therapy may provide enhanced regenerative effects. However, most previous studies have evaluated these modalities separately or in clinical settings where outcomes may be influenced by patient variability and external factors.(13,14) Their combined effects have not been adequately investigated in controlled experimental models of oxidative stress–mediated skin aging, particularly using validated D-galactose–induced aging models.

Therefore, this study was conducted to evaluate the effects of combined RFM and PDO filler therapy in a D-galactose-induced oxidative stress model of skin aging. Specifically, this study compared the effects of RFM monotherapy, PDO monotherapy, and combination therapy on dermal thickness, collagen density, and fibroblast count. These histological parameters were used to assess the regenerative effects of the treatments and to determine whether combination therapy provides additional benefits compared with monotherapy in aged skin.

Methods

This *in vivo* study used a randomized, controlled design with endpoint histological analysis to evaluate single and combined therapies in oxidative stress-mediated skin aging. Thirty healthy female Sprague-Dawley rats (*Rattus norvegicus*), aged 8–9 weeks and weighed 180–200 g, were used. Female rats were chosen to control for sex-based hormonal variation in skin physiology and wound healing. (15) Animals were housed under controlled conditions: 12 hour light/dark cycle, temperature 22–24°C, humidity 40-60%" with "a 12-hour light/dark cycle, a temperature of 22–24°C, and humidity of 40–60%, with ad libitum access to standard rodent diet (HPS 511) and filtered water.(16)

D-Galactose-Induced Aging Model

Systemic aging was induced via daily intraperitoneal injection of D-galactose (Sigma-Aldrich St. Louis, MO, United States) at 50 mg/kg body weight for 8 consecutive weeks. This model accelerates aging through oxidative stress and advanced glycation end-product formation, resulting in dermal thinning and collagen degradation. This dose and duration have been reported to effectively induce these histological features within an experimentally feasible timeframe while maintaining animal viability and model consistency.(17,18)

Rats were randomly allocated into five groups (n=5): group 1 (NC): Normal control (no D-galactose, no treatment); group 2 (AC): Aging model (D-galactose only, no treatment), group 3 (RFM): D-galactose + RFM monotherapy, group 4 (PDO): D-galactose + PDO filler monotherapy, group 5 (RFM+PDO): D-galactose + RFM + PDO filler (combination). Dorsal hair was shaved in a 1×1 cm area prior to procedures. After completion of the 8-week D-galactose induction period, therapeutic interventions were performed once on the first day of week-9 (Table 1, Figure 1).

Therapeutic Interventions

All procedures were performed under general anesthesia (35 mg/kg ketamine + 5 mg/kg xylazine, i.m.). RFM was performed using a bipolar device Ellisys Sense (Chungwoo Medical, Seoul, South Korea) with a 25-pin tip at 1.5 mm depth, 2 MHz, 40% intensity, 25W power, and 200 ms treatment time. A single pass was applied to a 1 cm^2 treatment area.(19) Meanwhile, PDO filler was administered using Ultra V® UltraCol 200 (Ultra V Co., Ltd., Seoul, South Korea). A volume of 10 mg/mL was injected into the mid-dermal layer via 32-gauge needle as multiple micro-depots.(20) In the combination group, PDO was injected immediately after RFM to utilize the microchannels created by microneedling for dermal delivery. All procedures were performed in accordance to the ethically approved protocol.

Table 1. Demographic and experimental overview of study subjects.

Group (n=5)	D-gal Induction	Therapeutic Intervention	Primary Objective
Normal Control (NC)	None	None	Baseline histology of normal skin
Aging Model (AC)	50 mg/kg/day i.p. for 8 weeks	None	Confirm establishment of aging phenotype
RFM Monotherapy (RFM)	50 mg/kg/day i.p. for 8 weeks	RFM once at week 9	Evaluate efficacy of RFM alone
PDO Monotherapy (PDO)	50 mg/kg/day i.p. for 8 weeks	PDO filler injection (10 mg/mL) once at week 9	Evaluate efficacy of PDO filler alone
Combination Therapy (RFM+PDO)	50 mg/kg/day i.p. for 8 weeks	RFM followed by PDO filler once at week 9	Evaluate synergistic efficacy of combined therapy

Tissue Harvesting and Histology

All animals were euthanized in the 12th week, or 4 weeks after treatment. This timepoint was selected based on established wound healing timelines where the neocollagenesis and extracellular matrix reorganization peak during the remodeling phase in rodent models, typically at 3–4 weeks post-injury, allowing for stable assessment of architectural restoration. Full-thickness skin samples were taken via 4 mm punch biopsy, fixed in formalin, processed, and embedded in paraffin. Sections as much as 5 µm were stained with Hematoxylin & Eosin (H&E) (21) and Masson's Trichrome (22).

Histomorphometric Analysis

A blind observer performed quantitative analysis using light microscopy and image analysis software Image Raster (Informer Technologies, Inc., Los Angeles, CA, USA). Parameters measured included: dermal thickness (µm): from stratum basale to dermal-fat junction (5 measurements/ sample) (23); collagen density (%): area of blue-stained collagen relative to total dermal area in Masson's Trichrome sections (5 fields/sample); and fibroblast count (cells/field): spindle-shaped cells in dermis counted in standardized 50×50 µm grids (5 fields/sample) (24).

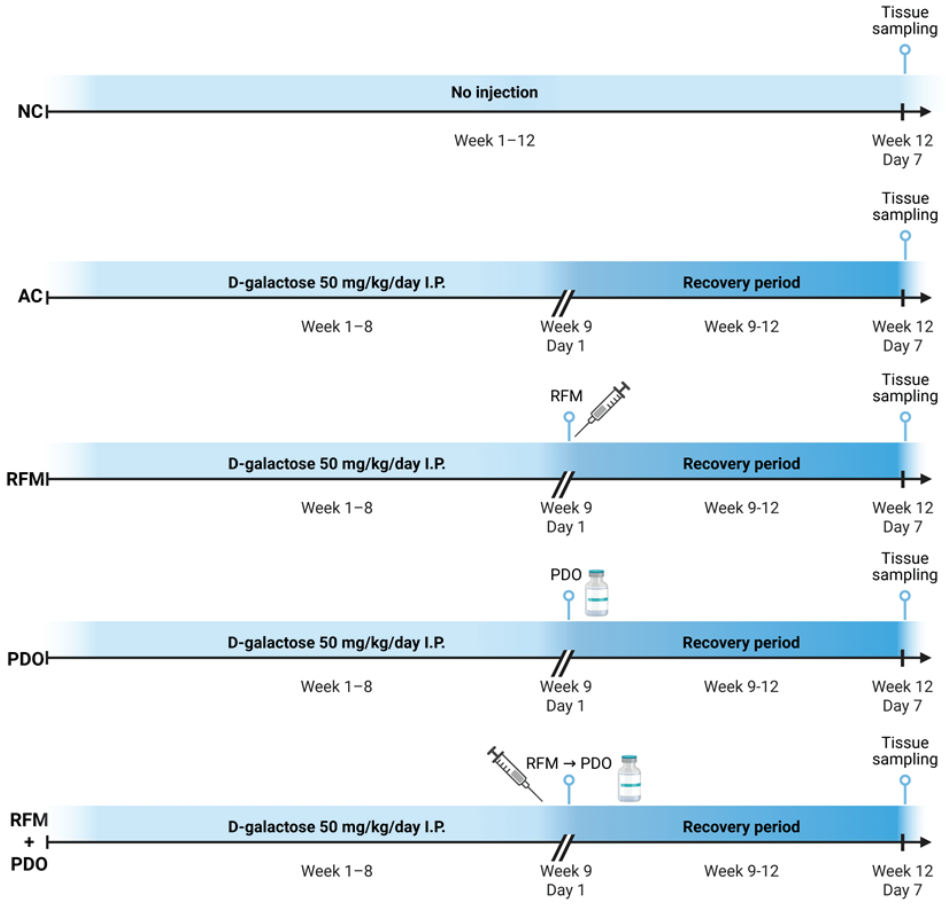

Figure 1. The experimental timeline and group design.

Statistical Analysis

Data were systematically coded and statistically analyzed utilizing SPSS software (IBM Corporation, Armonk, NY, USA). A p-value<0.05 was considered statistically significant.

Results

Chronic administration of D-galactose successfully induced structural and cellular alterations characteristic of skin aging. Histological examination using H&E staining demonstrated marked dermal degeneration in the AC group compared with the NC, including dermal compaction and disruption of the papillary–reticular architecture (Figure 2). Masson's trichrome staining further revealed a pronounced loss of collagen fibers in AC, characterized by sparse and fragmented collagen bundles (Figure 3). In parallel, fibroblast populations were markedly reduced in the aging model. Collectively, these findings confirm the successful establishment of a D-galactose–induced skin aging model that mimics oxidative stress–associated dermal degeneration.

Combination Therapy Showed the Highest Dermal Thickness Among Treatment Groups

Quantitative histomorphometric analysis confirmed significant alterations in dermal thickness across experimental groups (Figure 2F, Table 2). The AC group showed a significant reduction in dermal thickness compared with the NC group, indicating dermal atrophy following D-galactose administration.

The histological evaluation results demonstrated that all treatment interventions mitigated dermal thinning induced by aging. Representative H&E-stained sections showed partial to near-complete restoration of dermal architecture in the treatment groups (RFM, PDO, RFM+PDO), with improved organization of the papillary and reticular dermal layers (Figure 2C, 2D, and 2E). Post-hoc analysis indicated that dermal thickness was significantly increased in all treatment groups compared with the AC group (Table 2). Median dermal thickness values were 611.59 [595.84–676.00] µm in the RFM group, 633.55 [620.50–682.04] µm in the PDO group, and 764.70 [666.83–770.22] µm in the RFM+PDO group. Among the 3 treatment groups, the combination therapy demonstrated the highest dermal thickness and approached levels observed

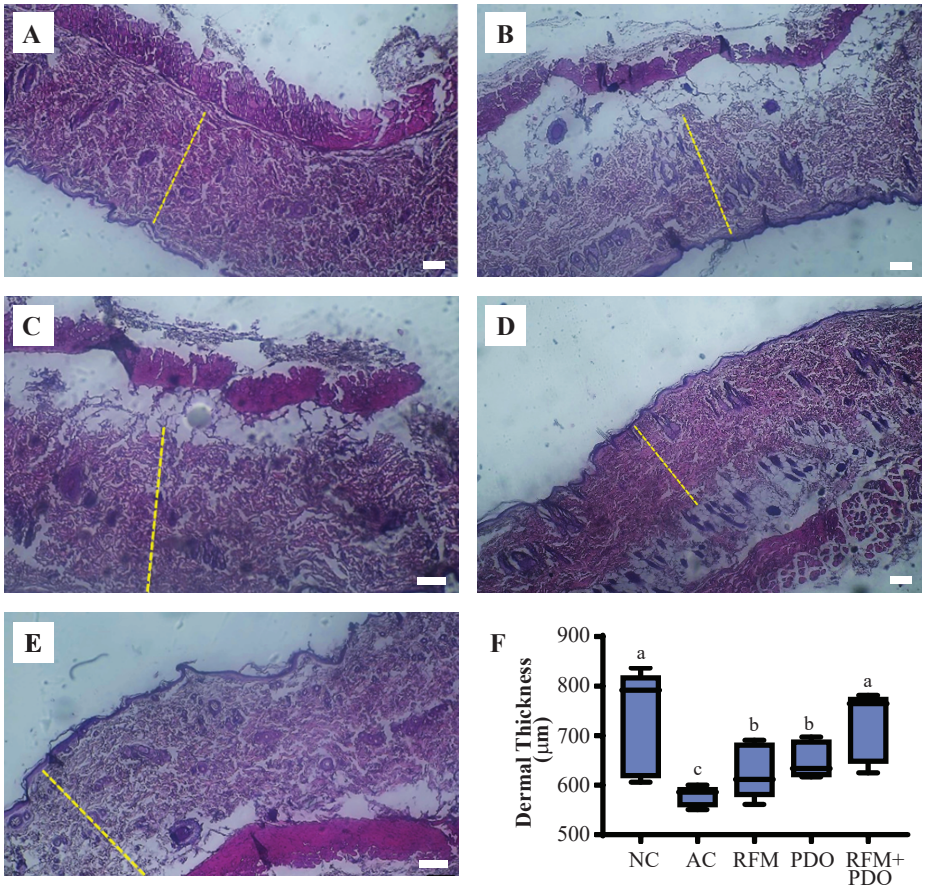

Figure 2. Dermal thickness of subjects in different experimental groups. A-E: Representative histological morphology examined using H&E staining (A: NC; B: AC; C: RFM, D: PDO, E: RFM+PDO). Yellow lines indicate the measurement of dermal thickness. White bar: 100 µm. F: Quantitative analysis of dermal thickness (µm). Data are presented in median and interquartile range (IQR). Statistical analysis was performed using the Kruskal–Wallis test followed by the Mann–Whitney U test. Different superscript letters indicate statistically significant differences between groups (p<0.05).

Table 2. Comparative histomorphometric outcomes across groups.

Variable	Group (n=5)	Value	Overall *p*-value	Post hoc comparison (*vs.* AC)
Dermal Thickness (μm)	NC	791.61 [627.28–801.75]	<0.001	—
	AC	585.85 [565.32–587.24]		—
	RFM	611.59 [595.84–676.00]		0.012*
	PDO	633.55 [620.50–682.04]		0.008*
	RFM+PDO	764.70 [666.83–770.22]		0.002*
Collagen Density (%)	NC	37.83 [33.11–40.69]	<0.001	—
	AC	7.67 [6.57–8.70]		—
	RFM	22.33 [20.30–23.74]		<0.001*
	PDO	24.09 [23.91–26.47]		<0.001*
	RFM+PDO	35.22 [28.74–40.35]		<0.001*
Fibroblast Count (cells/field)	NC	7683.60±990.54	<0.001	—
	AC	4202.40±851.29		—
	RFM	5694.40±1108.97		0.010*
	PDO	6244.56±1237.11		0.006*
	RFM+PDO	7005.72±976.55		0.001*

Data are presented as median and interquartile range (IQR) for dermal thickness and collagen density, and as mean±standard deviation (SD) for fibroblast counts. Dermal thickness and collagen density were analyzed using the Kruskal–Wallis test followed by the Mann–Whitney U test for pairwise comparisons. Fibroblast counts were analyzed using one-way ANOVA followed by Tukey's post hoc test. *p<0.05 *vs*. aging control (AC).

in the NC group, although the differences between the combination therapy and monotherapy groups were not statistically significant.

Combination Therapy Restored Collagen Density Comparable to Normal Skin

Masson's trichrome staining results demonstrated a clear treatment-dependent restoration of dermal collagen architecture (Figure 3). In the untreated aging model (AC group), collagen fibers appeared sparse, fragmented, and poorly organized, consistent with severe extracellular matrix degradation (Figure 3B). Both RFM and PDO monotherapies resulted in visible improvements in collagen fiber distribution and continuity; however, collagen networks remained less dense and less organized compared with normal skin (Figure 3C and 3D). Quantitative analysis demonstrated that collagen density was significantly increased in all treatment groups compared with the AC group (Figure 3F, Table 2). In particular, the combination therapy group demonstrated the highest collagen density (35.22 [28.74–40.35]%), which was significantly higher than both monotherapy groups and was not significantly different from the NC group. These findings indicate near-complete restoration of dermal collagen architecture with combination therapy.

Combination Therapy Showed the Highest Fibroblast Count Among Treatment Groups

Quantitative analysis revealed a marked reduction in fibroblast populations in the AC group compared with NC (p<0.001), confirming cellular depletion associated with oxidative stress–induced aging (Figure 4). All treatment interventions significantly attenuated fibroblast loss. Fibroblast counts were 5694.40±1108.97 cells/field in the RFM group, 6244.56±1237.11 cells/field in the PDO group, and 7005.72±976.55 cells/field in the combination therapy group (Table 2). Among the treated groups, the combination therapy exhibited the highest fibroblast count and approached levels observed in the NC group. However, differences between combination therapy and monotherapy groups did not reach statistical significance.

Discussion

This study demonstrates that the combination of RFM and PDO filler enhances restoration of dermal collagen architecture in an oxidative stress–mediated skin aging model compared with monotherapy. Using a validated D-galactose–induced aging model (25), only the combination treatment was observed to restore collagen

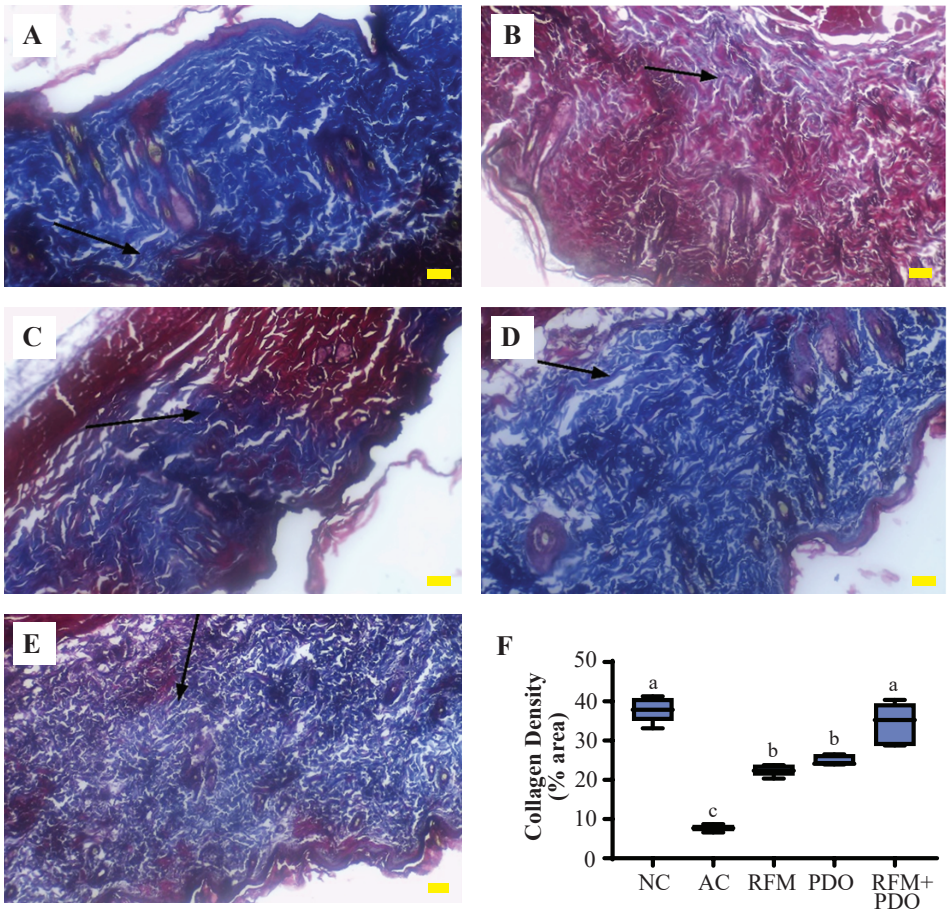

Figure 3. Collagen density of subjects in different experimental groups. A-E: Representative histological morphology examined using Masson's trichrome staining (A: NC; B: AC; C: RFM, D: PDO, E: RFM+PDO). Collagen fibers are stained blue. Black arrows indicate collagen fiber bundles in the dermal layer. Yellow bar: 100 µm. F: Quantitative analysis of collagen density (% area). Data are presented in median and interquartile range (IQR). Statistical analysis was performed using the Kruskal–Wallis test followed by the Mann–Whitney U test. Different superscript letters indicate statistically significant differences between groups (p<0.05).

density to levels statistically comparable to those of normal, non-aged skin. In contrast, monotherapies, while significantly improving collagen content, did not achieve full normalization. These findings support the emerging concept that rationally designed combination therapies may offer enhanced regenerative outcomes in dermatologic interventions.(10,11) Similar improvements in collagen regulation, fibroblast activity, and anti-aging responses under oxidative or aging-related conditions have been reported in previous experimental studies, supporting the biological relevance of collagen-focused regenerative interventions.(26-28)

The aging model used in this study successfully reproduced hallmark features of dermal aging, including significant dermal thinning, marked collagen depletion, and reduced fibroblast populations. Both RFM and PDO monotherapies significantly improved these alterations, confirming their intrinsic regenerative capacities even within an oxidative microenvironment. RFM is known to induce neocollagenesis through controlled thermal and mechanical stimulation, activating wound-healing cascades and fibroblast activity (6), as well as increasing the expression of growth factors such as transforming growth factor (TGF)-β and epidermal growth factor (EGF). In experimental models, the density of collagen types I and III significantly increases following RFM, indicating structural changes in the dermis consistent with skin regeneration, and the regulation of matrix metalloproteinases (MMPs) supports dermal matrix remodeling through fibroblast activation. (7) Additionally, RFM is effective in inducing progressive dermal remodeling and neocollagenesis, with effects that continue to develop for several months after treatment.(6) In line with this, clinical and histological evaluations in humans have shown increases in collagen and elastin in the dermis several months after RFM application, supporting the biological potential of this method for restoring collagen architecture in aging skin.(29) Meanwhile, PDO acts as a biostimulatory scaffold that supports sustained collagen synthesis and extracellular matrix remodeling. (8) The observed improvements in dermal thickness, collagen density, and fibroblast counts indicate that each modality remains biologically active under oxidative stress conditions, thereby establishing a necessary foundation for evaluating potential synergistic effects.

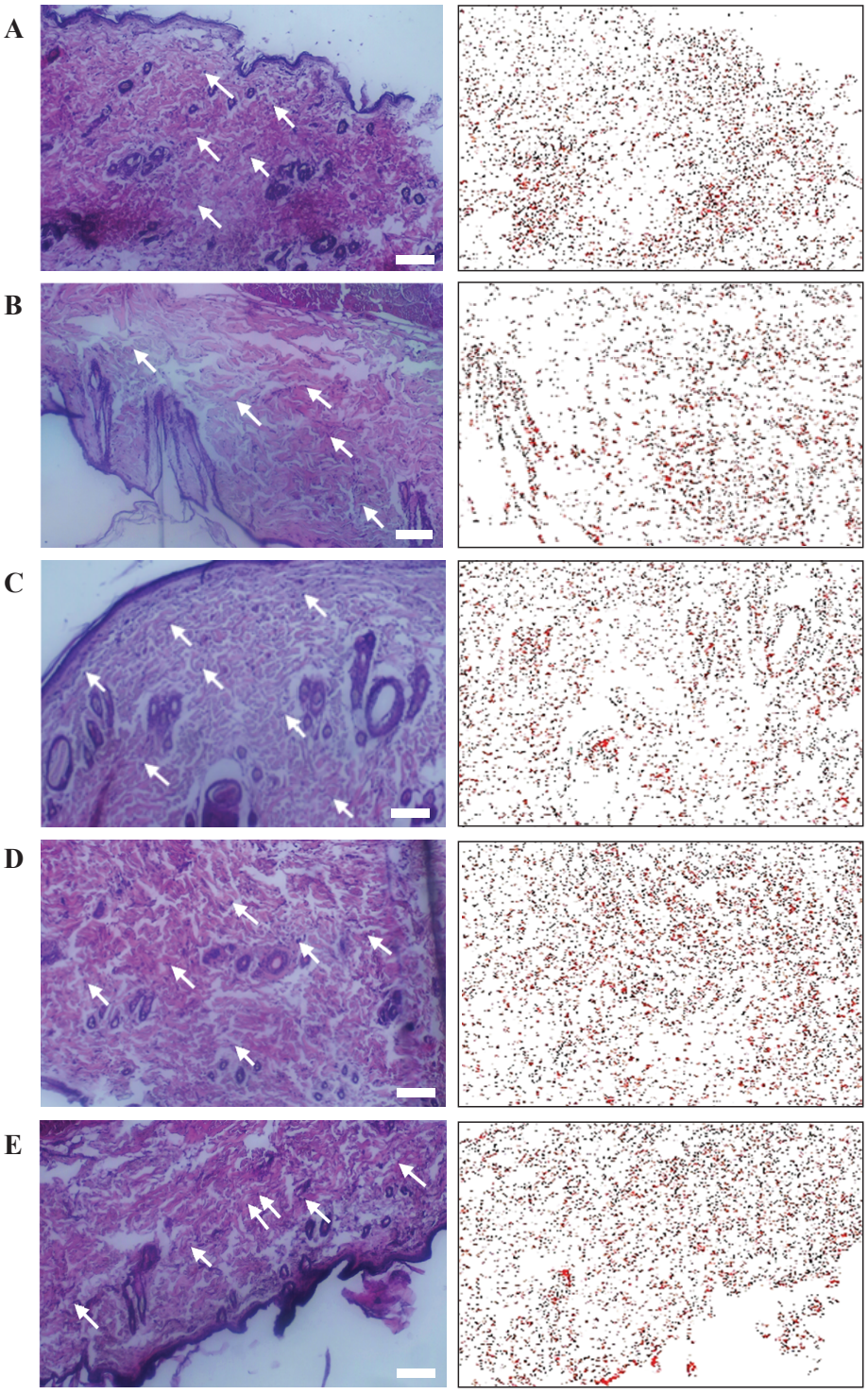

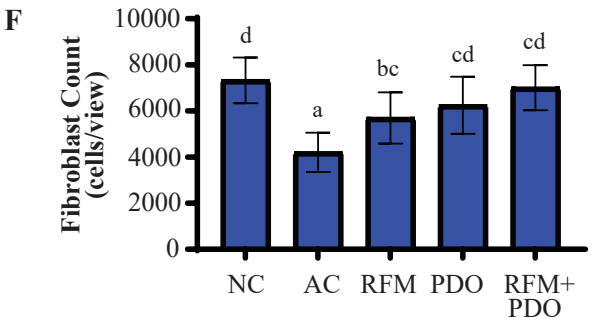

Figure 4. Fibroblast count of subjects in different experimental groups. A-E: Representative histological morphology examined using H&E staining and quantitative fibroblast analysis was performed using digital image analysis (A: NC; B: AC; C: RFM, D: PDO, E: RFM+PDO). White arrows indicate fibroblast cells (left), where detected fibroblast nuclei are highlighted in red (right). White bar: 100 µm. F: Quantitative analysis of fibroblast count (cells/view). Data are presented in mean±SD. Statistical analysis was performed using One-way ANOVA followed by Tukey's post hoc test. Different superscript letters indicate statistically significant differences between groups (p<0.05).

Among all treatment groups, the combination therapy produced the most pronounced improvement in collagen density, achieving near-complete restoration to normal levels. While dermal thickness and fibroblast counts also increased, these parameters did not differ significantly from those observed in the monotherapy groups, suggesting overlapping contributions of each treatment modality. Aging is associated with mitochondrial dysfunction, stem cell senescence, and impaired fibroblast activity, which collectively reduce extracellular matrix regeneration under oxidative stress conditions.(30-32) The enhanced collagen restoration observed in the combination group may reflect complementary mechanisms, in which RFM induces micro-injury and growth factor release, thereby priming the dermal microenvironment, while PDO filler provides structural support that sustains collagen synthesis and extracellular matrix remodeling.(33) This proposed dual-signal mechanism, integrating immediate injury-induced regeneration with longer-term scaffold-mediated remodeling, may explain the enhanced collagen restoration observed in the combination therapy group and is consistent with principles of tissue engineering and regenerative medicine, although direct mechanistic validation is still required.(34) RFM induces controlled microinjury and thermal stimulation, promoting growth factor release and transient increases in dermal permeability. These effects may enhance PDO filler distribution and cellular interaction, enabling sustained biostimulatory signaling and prolonged collagen synthesis. The integration of acute injury–driven regeneration and chronic scaffold-mediated remodeling may underlie the observed synergistic restoration of dermal collagen architecture.

The present findings provide a preclinical rationale for the use of combined RFM–PDO protocols in managing intrinsic and oxidative skin aging, extending beyond traditional photoaging models. From a clinical perspective, these results support structured combination treatment strategies rather than isolated interventions, particularly in cases characterized by advanced collagen depletion. Furthermore, the data underscores the importance of evidence-based approaches in the development, regulation, and education surrounding combination therapies in aesthetic and regenerative dermatology.

The evaluation performed in this study was limited to histomorphometric parameters without molecular analyses, which restricts mechanistic interpretation. In addition, although the D-galactose model reflects oxidative stress–related aging, it does not fully represent the complexity of human skin aging. The use of a single treatment session and a single post-treatment time point also adds limitation in the assessment of temporal and cumulative regenerative responses, as repeated treatments may produce different effects. At last, as a preclinical study with a relatively small sample size, caution is needed in extrapolating these findings to clinical settings. Further studies incorporating molecular endpoints, longitudinal evaluation, repeated treatment protocols, and clinical validation are warranted. This work moves beyond anecdotal combination practices, offering a mechanistic, evidence-based rationale for integrated treatment protocols in clinical practice. Combined RFM and PDO filler should be considered a more effective paradigm for addressing profound collagen depletion in both intrinsic and oxidative skin aging, with significant potential to improve outcomes in regenerative dermatology.

Conclusion

This study demonstrates that the strategic combination of RFM and PDO filler improved dermal structural parameters in a D-galactose–induced oxidative stress model of skin aging. Both monotherapies significantly enhanced dermal thickness, collagen density, and fibroblast counts, but the combination therapy showed the greatest improvement in collagen density. These findings suggest that combining RFM and PDO filler may enhance dermal collagen restoration under oxidative stress conditions in this preclinical model.

Acknowledgments

The authors extend their sincere gratitude to the Faculty of Medicine, Maranatha Christian University for the provision of the Maranatha Biomedical Research Laboratory (MBRL) and its research facilities. We also wish to acknowledge the technical staff of the Animal Laboratory for their diligent care of the experimental subjects and adherence to ethical husbandry protocols throughout the study. This research was supported by the Master's Program in Skin Aging and Aesthetic Health, Faculty of Medicine, Maranatha Christian University. The authors declare that no additional external funding was received for this specific work.

Authors Contribution

RAS was responsible for conceptualizing and designing the study, conducting the experiments, performing data

acquisition and analysis, as well as drafting the manuscript and preparing the figures. CP and WW contributed as supervisors by providing guidance on the research design, assisting in data interpretation, and critically revising the manuscript for important intellectual content. All authors reviewed and approved the final version of the manuscript.

Ethical Statement

The protocol was approved by the Health Research Ethics Committee, Faculty of Medicine, Maranatha Christian University (Ethical Approval No. 171/KEP/VII/2025).

Conflict of Interest

Authors declare no conflict of interest.

References

1. Russell-Goldman E, Murphy GF. The pathobiology of skin aging. Am J Pathol. 2020; 190(7): 1356-69.
2. Gu Y, Han J, Jiang C, Zhang Y. Biomarkers, oxidative stress and autophagy in skin aging. Ageing Res Rev. 2020; 59: 101036. doi: 10.1016/j.arr.2020.101036.
3. Azman KF, Zakaria R. D-Galactose-induced accelerated aging model: An overview. Biogerontology. 2019; 20(6): 763-82.
4. Umbayev B, Askarova S, Almabayeva A, Saliev T, Masoud AR, Bulanin D. Galactose-induced skin aging: the role of oxidative stress. Oxid Med Cell Longev. 2020; 2020: 7145656. doi: 10.1155/2020/7145656.
5. Ho SC, Liu JH, Wu RY. Establishment of the mimetic aging effect in mice caused by D-galactose. Biogerontology. 2003; 4(1): 15-8.
6. Tan MG, Jo CE, Chapas A, Khetarpal S, Dover JS. Radiofrequency microneedling: A comprehensive and critical review. Dermatol Surg. 2021; 47(6): 755-61.
7. Xu Y, Zhang Y, Wang H, Tang H, Zeng W, Wen X. Microneedle radiofrequency induces extracellular matrix remodeling through fibroblast activation: a histological study in a porcine model. Lasers Surg Med. 2025; 57(6): 528-43.
8. Kwon T, Han SW, Yeo IK, Kim JH, Kim JM, Hong J, *et al.* Biostimulatory effects of polydioxanone, poly-d,l-lactic acid, and polycaprolactone fillers in mouse model. J Cosmet Dermatol. 2019; 18(4): 1002-8.
9. Zhou SY, Kang SM, Gu YJ, Zhang XR, Yon DK, Shin BH, *et al.* Bio-characteristics and efficacy analysis of biodegradable poly dioxanone dermal filler in a mouse model and humans. In Vivo. 2023; 37(3): 1093-102.
10. Jin Y, Lee YH, Kim DH, Jin C, Zhang X, Yoo JR, *et al.* Synergistic CO_2 cryotherapy and EGF delivery for accelerated wound healing through anti-inflammatory and regenerative pathways. Int J Mol Sci. 2025; 26(18): 8796. doi: 10.3390/ijms26188796.
11. Song H, Fu F, Chen Y, Yang R, Luo Z, Shao J, *et al.* A poly(lipoic acid)-based elastomer adhesive with synergistic activity of microenvironment regulation and peripheral neuropathy repair facilitates infectious diabetic wound healing. Biomaterials. 2026; 324: 123489. doi: 10.1016/j.biomaterials.2025.123489.
12. Wu X, Cen Q, Wang X, Xiong P, Wu X, Lin X. Microneedling radiofrequency enhances poly-L-lactic acid penetration that effectively improves facial skin laxity without lipolysis. Plast Reconstr Surg. 2024; 154(6): 1189-97.
13. Seo KY, Yoon MS, Kim DH, Lee HJ. Skin rejuvenation by microneedle fractional radiofrequency treatment in Asian skin; clinical and histological analysis. Lasers Surg Med. 2012; 44(8): 631-6.
14. Kim H, Park KY, Choi SY, Koh HJ, Park SY, Park WS, *et al.* The efficacy, longevity, and safety of combined radiofrequency treatment and hyaluronic acid filler for skin rejuvenation. Ann Dermatol. 2014; 26(4): 447-56.
15. Sgonc R, Gruber J. Age-related aspects of cutaneous wound healing: A mini-review. Gerontology. 2013; 59(2): 159-64.
16. Russell WMS, Burch RL. The Principles of Humane Experimental Technique. London: Methuen; 1959.
17. Chen J, Li Y, Zhu Q, Li T, Lu H, Wei N, *et al.* Anti-skin-aging effect of epigallocatechin gallate by regulating epidermal growth factor receptor pathway on aging mouse model induced by d-galactose. Mech Ageing Dev. 2017; 164: 1-7. doi: 10.1016/j.mad.2017.03.007.
18. Wang H, Wei S, Xue X, You Y, Ma Q. Adipose stem cells' antagonism in glycosylation of D-galactose-induced skin aging of nude mice and its skin recovery function. Int J Immunopathol Pharmacol. 2016; 29(3): 376-85.
19. Kim HK, Kim HJ, Kim JY, Ban MJ, Son J, Hwang Y, *et al.* Immediate and late effects of pulse widths and cycles on bipolar, gated radiofrequency-induced tissue reactions in in vivo rat skin. Clin Cosmet Investig Dermatol. 2023; 16: 721-9.
20. Kwon T, Han SW, Yeo IK, Kim JH, Kim JM, Hong J, *et al.* Biostimulatory effects of polydioxanone, poly-d,l-lactic acid, and polycaprolactone fillers in mouse model. J Cosmet Dermatol. 2019; 18(4): 1002-8.
21. Widowati W, Darsono L, Lucianus J, Setiabudi E, Obeng SS, Stefani S, *et al.* Butterfly pea flower (Clitoria ternatea L.) extract displayed antidiabetic effect through antioxidant, anti-inflammatory, lower hepatic GSK-3β, and pancreatic glycogen on diabetes mellitus and dyslipidemia rat. J King Saud Univ Sci. 2023; 35(4): 102579. doi: 10.1016/j.jksus.2023.102579.
22. Islam MA, Kumar S. Masson's trichrome staining technique to evaluate tissue fibrosis. In: Fibrosis: Methods and Protocols. New York: Humana Press; 2026. p.91-100.
23. Inforzato HCB, Carbonel AAF, Simões RS, da Silva Sasso GR, Azevedo Lima PD, Soares-Júnior JM, *et al.* Histomorphometric analysis of the skin of women during the reproductive period. Clinics. 2018; 73: e387. doi: 10.6061/clinics/2018/e387.
24. Utoyo FS, Widowati W, Ratnawati H. The potency of Centella asiatica leaf extract on VEGF expression and angiogenesis in second-degree burn wound in mice. Hayati J Biosci. 2025; 32(1): 140-6.
25. Mao GX, Zheng LD, Cao YB, Chen ZM, Lv YD, Wang YZ, *et al.* Antiaging effect of pine pollen in human diploid fibroblasts and in a mouse model induced by D-galactose. Oxid Med Cell Longev. 2012; 2012: 750963. doi: 10.1155/2012/750963.
26. Siswanto FM. Resveratrol protects Caenorhabditis elegans from ultraviolet B-induced photoaging via skn-1. Mol Cell Biomed Sci. 2025; 9(1): 48-57.
27. Girsang E, Lister IN, Ginting CN, Bethasari M, Amalia A, Widowati W. Comparison of antiaging and antioxidant activities of protocatechuic and ferulic acids. Mol Cell Biomed Sci. 2020; 4(2):

68-75.
28. Valentina I, Achadiyani A, Adi SS, Lesmana R, Farenia R. Effect of Lactobacillus reuteri administration on wrinkle formation and type I procollagen levels in UVB-exposed male Balb/c mice (Mus musculus). Mol Cell Biomed Sci. 2020; 4(3): 113-20.
29. Wang Q, Ma C, Zhang L. A scoping review of radiofrequency microneedling: clinical application and outcome assessment. Aesthetic Plast Surg. 2025; 49(18): 5199-210.
30. Meiliana A, Dewi NM, Wijaya A. Mitochondrial dysfunction in stem cell aging. Indones Biomed J. 2015; 7(1): 15-30.
31. Meiliana A, Dewi NM, Wijaya A. Stem cell quiescence versus senescence: the key for healthy aging. Indones Biomed J. 2021; 13(4): 337-49.
32. Dewi DA, Sandra F. Conditioned media of human umbilical cord blood mesenchymal stem cell inhibits ultraviolet B-induced apoptosis in fibroblasts. Indones Biomed J. 2019; 11(1): 85-90.
33. Wu X, Cen Q, Wang X, Xiong P, Wu X, Lin X. Microneedling radiofrequency enhances poly-L-lactic acid penetration that effectively improves facial skin laxity without lipolysis. Plast Reconstr Surg. 2024; 154(6): 1189-97.
34. Zhu Q, Zhu L, Lang J, Zhu J, Chen D, Huang Y, *et al.* Dopamine-functionalized bioinspired pre-chondrogenic hydrogel for cell-free cartilage regeneration. J Control Release. 2026; 389: 114407. doi: 10.1016/j.jconrel.2025.114407.